Archives of Materials Science and Engineering

Volume 79
Issue 1
May 2016
Pages 27-36

International Scientific Journal
published monthly by the
World Academy of Materials
and Manufacturing Engineering

Parametric optimization of MIG welding on 316L austenitic stainless steel by Taguchi method

N. Ghosh *, P.K. Pal, G. Nandi
Mechanical Engineering Department, Jadavpur University, Kolkata 700032,W.B, India
* Corresponding e-mail address: nabendu2003_ghosh@yahoo.co.in

ABSTRACT

Purpose: Taguchi design has been adopted in order to identify optimal parametric combination for desired quality of weld.

Design/methodology/approach: A plan of experiments based on Taguchi technique has been used. An orthogonal array, signal to noise (S/N) ratio and analysis of variance (ANOVA) are employed to study the welding characteristics of material & optimize the welding parameters.

Findings: The welding investigators have always been in search for better quality of weldment. In present work, effect of current, gas flow rate and nozzle to plate distance on quality of weld in metal gas arc welding of Austenitic stainless steel AISI 316L has been studied through experiment and analyses. Butt welded joints have been made by several levels of current, gas flow rate and nozzle to plate distance. The result computed is in form of contribution from each parameter, through which optimal parameters are identified for maximum tensile strength and percentage elongation.

Research limitations/implications: The main objective of the present study was to apply the Taguchi method to establish the optimal set of control parameters for the welding. The Taguchi method is employed to determine the optimal combination of design parameters, including: current, gas flow rate and nozzle to plate distance.

Practical implications: Weld quality mainly depends on features of bead geometry, mechanical-metallurgical characteristics of the weld as well as on various aspects of weld chemistry and these features are expected to be greatly influenced by various input parameters like current, voltage, electrode stick-out, gas flow rate, edge preparation, position of welding, welding speed and many more in metal inert gas (MIG) welding. Moreover, the cumulative effect of the mentioned quality indices determines the extent of joint strength that should meet the functional aspects of the weld in practical field of application. Therefore, preparation of a satisfactory good quality weld seems to be a challenging job.

Originality/value: The result computed is in form of contribution from each parameter, through which optimal parameters are identified for maximum tensile strength and percentage elongation. This paper presents new results of optimization using Taguchi method.

Keywords: MIG welding; AISI 316L austenitic stainless steel; X-ray radiographic test; Tensile test; Taguchi method; ANOVA; Signal to noise (S/N) ratio; Optimization

Reference to this paper should be given in the following way:

N. Ghosh, P.K. Pal, G. Nandi, Parametric optimization of MIG welding on 316L austenitic stainless steel by Taguchi method, Archives of Materials Science and Engineering 79/1 (2016) 27-36.

MATERIALS MANUFACTURING AND PROCESSING

1. Introduction

Welding of austenitic stainless steel in general, and MIG welding of such steel in particular, can well be considered as one of the areas where more extensive research may contribute, in a significant way, to the precise control of welding procedure for better and acceptable quality of weldment.

Researchers had done investigations on joining the 316L austenitic stainless steel materials with use of MIG welding technique, those are discussed below: Kanjilal, T.K. Pal, S.K. Majumdar [1] developed a rotatable designs based on statistical experiments for mixtures to predict the combined effect of flux mixture and welding parameters on submerged arc weld metal chemical composition and mechanical properties.. P.K. Palani, N. Murugan [2] investigated the effect of cladding parameters such as welding current, welding speed, and nozzle-to-plate distance on the weld bead geometry.

The experiments were conducted for 317L flux cored stainless steel wire of size 1.2 mm diameter with IS:2062 structural steel as a base plate. A.K. Lakshminarayanan, V. Balasubramanian [3] investigated the microstructure analysis and mechanical properties evaluation of laser beam welded AISI 409M ferritic stainless steel joints. M. Mukherjee and T.K. Pal [4] described The effect of heat input on martensite formation and impact properties of gas metal arc welded modified ferritic stainless steel (409M) sheets (as received) with thickness of 4 mm. Eslam Ranjbamode [5] studied the microstructural characteristics of tungsten inert gas (TIG) welded AISI 409 ferritic stainless steel and effect of the welding parameters on grain size local mis-orientation and low angle grain boundaries was investigated. Hu et al [6] employed a high-precision magnetic sensor to detect the weld defects in aluminium friction stir welds. Lee et al. [7] have used the Taguchi method and regression analysis in order to optimize Nd-YAG laser welding parameters.

Laser butt-welding of a thin plate of magnesium alloy using the Taguchi method has been optimized by Pan et al. [8] Ibrahim et al. [9] investigated the effects of robotic GMAW process parameters on welding penetration, hardness and microstructural properties of mild steel weldments of 6 mm plate thickness. Murugan and Parmar [10] used a four-factors 5-levels factorial technique to predict the weld bead geometry (penetration, reinforcement, width and dilution %) in the deposition of 316L stainless steel onto structural steel IS2062 using the MIG welding process. Rosado et al [11] utilized the eddy currents probe to detect the imperfections in friction stir welds of aluminium. Senthil Kumar et al. [12] developed mathematical models by regression analysis to predict the effects of pulsed current tungsten inert gas welding parameters on tensile properties of medium strength AA 6061 aluminium alloy. Seshank et al. [13] used ANN and Taguchi method to analyse the effect of pulsed current GTAW process parameters on bead geometry of aluminium bead-on plate weldment. Sittichai et al. [14] investigated the effects of shielding gas mixture, welding current and welding speed on the ultimate tensile strength and percentage elongation of GMA welded.

Sourav Datta et al. [15] used Taguchi approach followed by grey relational analysis to solve multi-response optimization problem in submerged arc welding. Juang and Tarng [16] have adopted a modified Taguchi method to analyse the effect of each welding process parameter (arc gap, flow rate, welding current and speed) on the weld pool geometry (front and back height, front and back width) and then to determine the TIG welding process parameters combination associated with the optimal weld pool geometry. Tarng and Yang [17] reported on the optimization of weld bead geometry in GTAW by using the Taguchi method. Tarng et al. [18] applied the modified Taguchi method to determine the process parameters for optimum weld pool geometry in TIG welding of stainless steel. Tarng et al. [19] also worked on the use of grey-based Taguchi method to determine optimum process parameters for submerged arc welding (SAW) in hard facing with consideration of multiple weld qualities.

Yilmaz and Uzun [20] compared the results obtained from destructive tests for mechanical properties of austenitic stainless steel. (AISI 304L and AISI 316L plates of 5 mm thickness) joints welded by GMAW and GTAW process. The joints were made by GMAW process using ER 316 L Si filler metal and by GTAW process using ER 308L and ER 316L filler metals. In the present work the effects of current, gas flow rate and nozzle to plate distance on ultimate tensile strengths, yield strength and percentage of elongation of butt-welded joints of austenitic stainless steel have been experimented and analysed through Taguchi method.

2. Experimental plan, set up and procedure

2.1. Experimental plan

Butt welding of AISI 316L austenitic stainless steel: 65 mm x 100 mm x 3 mm thick, have been done using the MIG welding machine make: ESAB AUTO K400.

Taguchi design has been adopted in order to identify optimal parametric combination for desired quality of weld. Total of 9 butt welded specimens have been obtained using

3 levels of current, 3 levels of gas flow rate and 3 level of nozzle to plate distance based on L9 Taguchi's Orthogonal Array Design of experiment. The interaction effects have not been considered in the present work. filler rod used has been ER 316L. Welding process parameters and their levels, and design matrix are shown in Table 1 and Table 2 respectively.

Table 1.
Welding process parameters and their levels (domain of experimentation) for L9 Taguchi's Orthogonal Array Design of experiment

			Levels		
Factors	Symbol	Unit	1	2	3
Welding current	C	A	100	112	124
Gas flow rate	F	l/min	10	15	20
Nozzle to plate distance	S	mm	9	12	15

Table 2.
Design matrix based on L9 Taguchi Orthogonal Array design of experiment chuck

	Welding parameters		
Sample No.	Welding current, A	Gas flow rate, l/min	Nozzle to plate distance, mm
1	1	1	1
2	1	2	2
3	1	3	3
4	2	1	2
5	2	2	3
6	2	3	1
7	3	1	3
8	3	2	1
9	3	3	2

2.2. Equipment and instruments used

Welding has been done on ESAB AUTO K 400 -MIG/MAG welding machine. X-ray radiographic tests have been conducted for all the samples by XXQ-2005 X-Ray flaw detector at SKB Metallurgical Services, Salkia, Howrah . Tensile tests have been carried out on Instron universal testing machine at Jadavpur University laboratory, kolkata, India using a hydraulic chuck. The photographic view of the ESAB AUTO K 400-MIG/MAG welding machine is shown in Figure 1.

Fig. 1. Photographic view of ESAB AUTO K-400 MIG/MAG welding machine

2.3. Experimental procedure

Welding set-up has been prepared, checked and made ready for doing welding. Butt joints are made by welding two pieces of austenitic stainless steel, grade AISI 316L. Each piece has the dimensions 65 mm x 100 mm x 3 mm. Nine welded samples are thus made, by carrying out welding at different levels of current, gas flow rate and nozzle to plate distance, as per Taguchi design of experiments, given in Table 2. Photographic view of a welded specimen is shown in Figure 2.

Fig. 2. Photographic view of a sample just after welding

After welding, visual inspection of the nine samples has been done. X-ray radiography tests are conducted next. Now tensile test specimens are made by machining the welded samples. During cutting/machining of the tensile test specimens, small size cut pieces also been made. This small size – cut pieces have then been ground, polished and etched

for studying microstructures. A schematic diagram showing the important dimensions of the tensile test specimens is given in Figure 3. Photographic view of tensile test specimen and Instron universal testing machine are shown in Figure 4 and Figure 5 respectively.

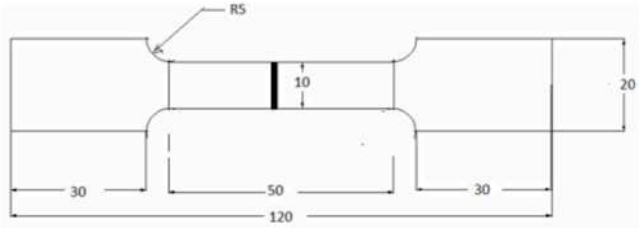

Fig. 3. Schematic diagram of the specimen prepared for tensile test

Fig. 4. Photographic view of tensile test specimen

Fig. 5. Instron universal testing machine

3. Results of X-ray radiographic tests of weldment and discussion

X-ray radiographic tests have been conducted for all the 9 samples by XXQ-2005 X-Ray flaw detector. Copies of X-radiographic film for few samples are shown in Figures 6 and 7. Result of X-ray radiographic test is shown in Table 3. Porosity in welding is caused by the presence of gases which get entrapped during the solidification process [21]. The most common causes of porosity are atmosphere contamination, excessively oxidized work piece surface, in add quote deoxidizing alloys in the wire and the presence of foreign matter, can be caused by Inadequate shielding gas flow, excessive shielding gas flow [25]. Most frequently the occurrence of lack of fusion due to an improper welding technology can be attributed to an improper preparation of a weld groove, an incorrect torch inclination, an improper welding position, and possible draught [22]. A second group of causes includes insufficient energy input to the weld area. It has been confirmed that it is highly important to choose optimum welding parameters such as welding current, wire feed rate, and arc length [23]. The welding speed has a major influence on energy input [24]. Welding current has the greatest effect on penetration. Incomplete penetration is usually caused by the use of too low welding current and can be eliminated by simply increasing the ampere. Other causes can be the use of too slow travel speed and an incorrect torch angle. Both will be allow the metal to rise in front of the arc acting as a cushion to prevent penetration. The arc must be kept on the leading edge of the weld puddle [25].

Table 3.
Result of X -ray radiographic tests

Sample No.	Result of X-ray radiographic tests
1	No defects
2	Lack of fusion, porosity
3	No defects
4	No defects
5	Porosity
6	No defects
7	Porosities
8	No defects
9	Porosities

Fig. 6. Copies of X-ray radiographic film for sample No. 01

Fig. 7. Copies of X-ray radiographic film for sample No. 07

4. Results of tensile test and discussion

The tensile test specimens, prepared corresponding to L9 Taguchi orthogonal array experiments, have been tested for tensile strengths and the results obtained are given in Table 4.

The Table 4 indicates that for many of the welded samples test results are satisfactory. The best result is obtained for the sample no.3 (Corresponding to current 100 A, flow rate 20 l/min and nozzle to plate distance 15 mm). For this sample yield strength = 322.74 MPa, ultimate tensile strength = 591.18 MPa, percentage of elongation = 54.54. The worst result in tensile testing has been obtained for the sample no. 7 (corresponding to current 124 A, gas flow rate 10 l/min and nozzle to plate distance 15 mm). For this sample yield strength = 242.43 MPa and ultimate tensile strength = 426.23 MPa and percentage of elongation = 19.52.

Table 4.
Tensile tests result as per L9 Taguchi orthogonal array design of experiment

Sample No.	Ultimate tensile strength, MPa	Percentage of elongation, %
Base plate	573.75	65.05
1	550.09	31.21
2	552.02	34.64
3	591.18	54.54
4	518.21	33.02
5	432.33	18.53
6	481.41	33.07
7	426.23	19.52
8	484.97	42.77
9	450.99	28.40

5. Taguchi method

Taguchi method is developed by Dr Genichi Taguchi, a Japanese scientist. Taguchi design of experiments provides an efficient and systematic way to optimize designs for performance, quality and cost. Taguchi method is widely used in different fields of engineering to optimize the manufacturing processes/systems. It is one of the most important tools for designing high quality systems/ processes at reduced cost. Taguchi method is based on orthogonal array experiments, emphasizes balanced design with equal weight age to all factors with less number of experimental runs. Therefore, cost as well as experimental time reduced drastically with orthogonal array of Taguchi method [17]. In order to evaluate the significance of process parameters, Taguchi method uses a statistical measure of performance called signal-to-noise (S/N) ratio that takes both the mean and the variability into account. The method explores the concept of quadratic quality loss function. The S/N ratio is the ratio of the mean (signal) to the standard deviation (noise). The ratio depends on the quality characteristics of the product/process to be optimized. The standard S/N ratios generally used are nominal-is-best (NB), lower-the-better (LB) and higher-the-better (HB).

Taguchi's S/N ratio for (NB) nominal-the-best

$$\eta = 10 \ln 10 \frac{1}{n} \sum_{i=1}^{n} \frac{\mu^2}{\sigma^2} \quad (1)$$

Taguchi's S/N ratio for (LB) lower-the-better

$$\eta = -10 \ln 10 \frac{1}{n} \sum_{i=1}^{n} y_i^2 \quad (2)$$

Taguchi's S/N ratio for (HB) higher-the-better

$$\eta = -10 \ln 10 \frac{1}{n} \sum_{i=1}^{n} \frac{1}{y_i^2} \quad (3)$$

5.1. Single objective optimization of Ultimate Tensile Strength (UTS) by Taguchi method

Taguchi method uses a statistical measure of performance called signal to noise (S/N) ratio. The S/N ratio is the ratio of the mean (Signal) to the standard deviation (Noise). It depends on the quality of the product or process. The standard S/N ratio used is as follows: nominal is the better, higher is the better and lower is the better. Maximization of both the responses is the requirement in the present work; hence higher is the better has been used. S/N ratios have been determined by using the eq.3.

The effect of process parameters on the performance is indicated by S/N ratio. Larger S/N ratio indicates that better signal is obtained and lesser noise is occurred. For each experimental run, corresponding S/N ratio is determined and listed in Table 5. Table 6 is the table corresponding to mean response table for ultimate tensile strength. Figure 8 shows the main effect plots. Mean S/N ratio table is given in Table 5. Main effect plots for S/N ratio are shown in Figure 9, using MINITAB 16 software.

Table 5.
Mean S/N ratio of UTS

Sample No.	Ultimate Tensile Strength, MPa	S/N ratio of UTS
1	550.09	54.81
2	552.02	54.84
3	591.18	55.43
4	518.22	54.29
5	432.34	52.72
6	481.41	53.65
7	426.23	52.59
8	484.97	53.71
9	450.99	53.08

Table 6.
Mean response table for ultimate tensile strength.

Level	Current, A	Gas flow rate, l/min	Nozzle to plate distance, mm
1	**564.4**	498.2	505.5
2	477.3	489.8	**507.1**
3	454.1	**507.9**	483.2
Delta	110.4	18.1	23.8
Rank	1	3	2

Figure 8 shows the effect of the different levels of parameters on the ultimate tensile strength.

Fig. 8. Main effect plots for mean of Ultimate Tensile Strength

The highest values are bold and underlined in Table 6:

- Level 1 for current (i.e. 100 A), resulting 564.4 MPa is indicated as the optimum condition in terms of ultimate tensile strength while variation of current is only considered;
- Level 3 for gas flow rate (i.e. 20 liter/minute), resulting 507.9 MPa is indicated as the optimum condition in terms of ultimate tensile strength while varying gas flow rate only;
- Level 2 for nozzle to plate distance (i.e. 12 mm), resulting in 507.1 MPa is indicated as the optimum condition in terms of ultimate tensile strength while varying nozzle to plate distance only.

Above observations can also be verified through S/N ratio plots where maximum S/N ratio is desired. Table 7 includes the data needed for S/N ratio plots. Highest values of S/N ratio are shown bold and underlined in this table. Main effect plots for S/N ratio of ultimate tensile strength are given in Figure 9.

Table 7.
Mean S/N ratio table for ultimate tensile strength

Level	Current, A	Gas flow rate, l/min	Nozzle to plate distance, mm
1	**55.03**	53.9	54.06
2	53.55	53.76	**54.07**
3	53.13	**54.06**	53.58
Delta	1.9	0.3	0.49
Rank	1	3	2

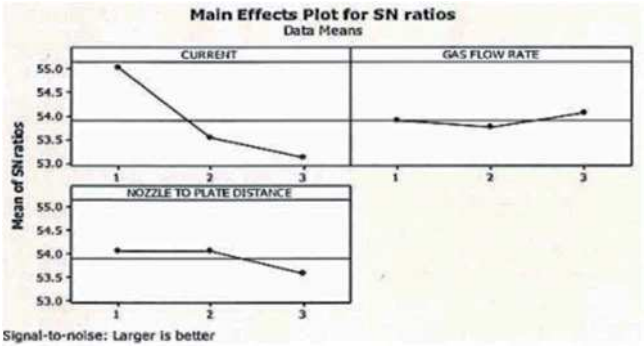

Fig. 9. Main effect plots for S/N ratio of Ultimate Tensile Strength

Higher the S/N ratio, smaller is the variance of the UTS towards the desired target (higher is the better). From Figure 9, it is found that current at level 1, gas flow rate at level 3 and nozzle to plate distance at level 2 [C1F3S2] (i.e. current 100 A, gas flow rate 20 liter/minute and nozzle to plate distance 12 mm) is the parametric condition which will give maximum value of ultimate tensile strength (UTS). Analysis of variance for ultimate tensile strength is shown in Table 8.

Analysis of variance (ANOVA) using MINITAB 16 software has been performed to determine the contribution of process parameters on ultimate tensile strength for Taguchi optimization method. From the Table 8 it is found that current is the most significant factor followed by nozzle to plate distance. Gas flow rate is not a very significant factor which influences UTS.

Confirmatory test

Confirmatory tests have been arranged and carried out to validate the above optimized condition. The results obtained are: UTS at optimized condition = 593.32 MPa. From the results of confirmatory test, it is found that optimum welding parametric condition produced maximum UTS, this value shows the validation of the proposed optimization methodology.

Table 8.
Analysis of variance for ultimate tensile strength

Source	DF	Seq SS	Adj SS	Adj MS	F	P	Percentage of contribution, %
Current	2	20309	20309	10155	4.09	0.197	75.6
Gas flow rate	2	491	491	246	0.1	0.91	1.8
Nozzle to plate distance	2	1065	1065	533	0.21	0.824	3.96
Error	2	4971	4971	2485			18.5
Total	8	26836					

DF = Degree of freedom

SS = Sum of sąuared deviation = $\sum_i^n (y_i - y)^2$

Where, y_i is the observed S/N ratio value of response, n is the number of observation or experiment number and y is the mean of S/N ratio. MS = Mean sauared deviation $= \frac{SS}{DF}$

F = Fisher test

(The terms used in all the ANOVA tables are the standard terms with usual significance).

Table 9.
Experimental observations and S/N ratios for percentage elongation (PE)

Sample No.	Percentage Elongation, %	S/N ratio of Percentage Elongation
1	31.21	29.89
2	34.64	30.79
3	54.54	34.73
4	33.02	30.38
5	18.53	25.36
6	33.07	30.39
7	19.52	25.81
8	42.77	32.62
9	28.40	29.07

5.2. Single objective optimization of Percentage Elongation (PE) by Taguchi method

Same procedure as discussed above is followed for optimization of percentage elongation (PE). The corresponding S/N ratio values are calculated and shown in Table 9.

Larger S/N ratio indicates that better signal is obtained and lesser noise is occurred. As higher is the better criterion is required, eq. 3. Mean response table for percentage elongation is shown in Table 10.

Table 10.
Mean response table for percentage elongation

Level	Current, A	Gas flow rate, l/min	Nozzle to plate distance, mm
1	**40.13**	27.92	**35.69**
2	28.21	31.98	32.02
3	30.23	**38.67**	30.86
Delta	11.92	10.75	4.82
Rank	1	2	3

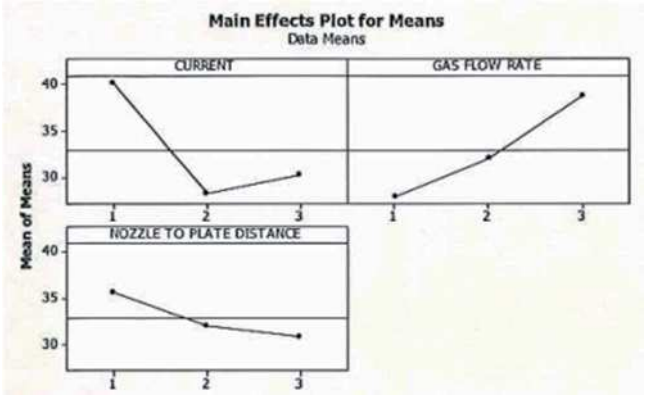

Fig. 10. Main effect plots for mean of percentage elongation

Figure 10 shows the effect of the different levels of the input parameters on percentage elongation. The highest values are shown bold and underlined in Table 10.

- Level 1 for current (i.e. 100 ampere), resulting 40.13% is indicated as the optimum condition in terms of percentage elongation while variation of current is only considered;
- Level 3 for gas flow rate (i.e. 20 liter/minute), resulting 38.67% corresponds to the optimum condition in terms of percentage elongation while varying gas flow rate only;
- Level 1 for Nozzle to plate distance (i.e. 9 mm), resulting in 35.69%, is found to be the optimum condition in terms of percentage elongation while varying nozzle to plate distance only.

Above observations can also be verified through S/N ratio plots where maximum S/N ratio corresponds to the optimum level. The response table for signal to noise ratio is shown in Table 11. Highest values of S/N ratio are shown bold and underlined in this table, and the corresponding main effect plots for S/N ratios are shown in Figure 11.

Table 11.
Mean S/N ratio table for percentage elongation

Level	Current, A	Gas flow rate, l/min	Nozzle to plate distance, mm
1	**31.8**	28.69	**30.97**
2	28.71	29.59	30.08
3	29.17	**31.4**	28.63
Delta	3.1	2.71	2.33
Rank	1	2	3

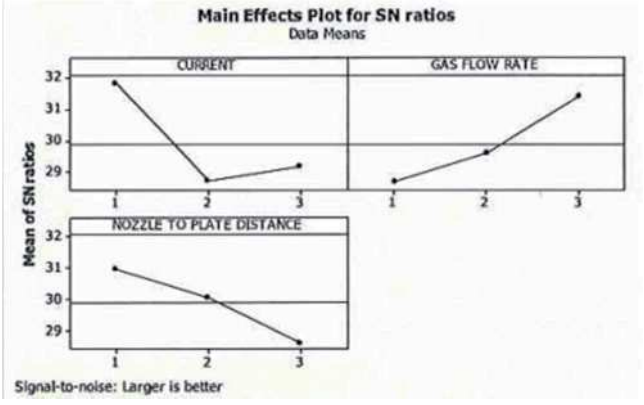

Fig. 11. Main effect plots for S/N ratio of percentage elongation

From the plots shown in Figure 11, the optimized condition for maximum percentage elongation is current at level 1, gas flow rate at level 3 and nozzle to plate distance at level 1 [C1F3S1] (i.e. current 100 A, gas flow rate 20 litre/min and nozzle to plate distance 9 mm), corresponding to the highest value of S/N ratio for each of these parameters. Analysis of variance for percentage elongation (PE) is shown in Table 12.

Analysis of variance (ANOVA) using MINITAB 16 software has been performed to determine the contribution of process parameters on ultimate tensile strength for Taguchi optimization method. From the Table 12 it is found that current is the most significant factor followed by gas flow rate. Nozzle to plate distance is not a very significant factor which influences UTS.

Table 12.
Analysis of variance for percentage elongation

Source	DF	Seq SS	Adj SS	Adj MS	F	P	Percentage of contribution, %
Current	2	244.2	244.2	122.1	0.47	0.68	24.9
Gas flow rate	2	176.8	176.8	88.4	0.34	0.75	18.0
Nozzle to plate distance	2	38	38	19	0.07	0.93	3.8
Error	2	518.2	518.2	259.1			53.0
Total	8	977.3					

Confirmatory test

Confirmatory tests have been arranged and carried out to validate the above optimized condition. The results obtained are: PE at optimized condition = 55.0%. From the results of confirmatory test, it is found that optimum welding parametric condition produced maximum PE, this value shows the validation of the proposed optimization methodology.

6. Conclusions

Following conclusions are drawn in respect of MIG welding of AISI 316L austenitic stainless steel:

- Results of X-ray radiography test indicate: lack of penetration, low – level porosity and lack of fusion in some of the samples.
- The best result is obtained for the sample no. 3 (corresponding to current 100 A, flow rate 20 l/min and nozzle to plate distance 15 mm). The worst result in tensile testing has been obtained for the sample no. 7 (corresponding to current 124 A, gas flow rate 10 l/min and nozzle to plate distance 15 mm).
- In single objective optimization by Taguchi, the objective is to maximize i) ultimate tensile strength (UTS) and ii) percentage elongation (PE) individually i.e. separately. Taguchi's S/N ratio concept is utilized and it is found that i) optimum condition for maximum UTS [C1F3S2] (i.e. current 100 A, gas flow rate 20 litre/minute and nozzle to plate distance 12 mm) ii) optimum condition for maximum PE is [C1F3S1] (i.e. current 100 A, gas flow rate 20 litre/min and nozzle to plate distance 9 mm).
- The optimum conditions determined by single-objective optimization techniques (Taguchi) have been validated by confirmatory tests.

Acknowledgements

The authors sincerely thanks all the staff members of Blue Earth workshop of Jadavpur University who directly or indirectly made their involvement in the experimental work and testing part of this work. The authors are very much grateful to SKB Metallurgical Services, Salkia, Howrah for their cooperation and help.

References

[1] P. Kanjilal, T.K. Pal, S.K. Majumdar, Combined effect of flux and welding parameters on chemical composition and mechanical properties of submerged arc weld metal, Journal of Materials Processing Technology 171 (2006) 223-231.

[2] P.K. Palani, N. Murugan, Sensitivity Analysis for Process Parameters in Cladding of Stainless Steel by Flux Cored Arc Welding, Journal of Manufacturing Processes 8/2 (2006) 90-100.

[3] A.K. Lakshminarayanan, V. Balasubramanian, Evaluation of Microstructure and Mechanical Properties of Laser Beam Welded AISI 409M Grade Ferritic Stainless Steel, Journal of Iron and Steel Research International 19/1 (2012) 72-78.

[4] M. Mukherjee, T.K. Pal, Influence of Heat Input on Martensite Formation and Impact Property of Ferritic-Austenitic Dissimilar Weld Metals, Journal of Materials Science Technology 28/4 (2012) 343-352.

[5] E. Ranjbarnodeh, Investigation of the Effect of Welding Parameters on HAZ of AISI409 Using EBSD, Journal of Material Science 2/1 (2010) 46-53

[6] B. Hu, R. Yu, H. Zou, Magnetic non-destructive testing methods for thin - plates aluminium alloys, NDT&E International 47 (2012) 66-69.

[7] H.K. Lee, H.S. Han, K.J. Son, S.B. Hong, Optimization of Nd-YAG laser welding parameters for sealing small titanium tube ends, Journal of Materials Science and Engineering A 415 (2006) 149-155.
[8] L.K. Pan, C.C. Wang, Y.C. Hsiso, K.C. Ho, Optimization of Nd-YAG laser welding onto magnesium alloy via Taguchi analysis, Journal of Optics and Laser Technology 37 (2004) 33-42.
[9] I.Z. Ibrahim, S.A. Mohama, A. Amir, A. Ghalib, The effect of Gas Metal Arc Welding (GMAW) processes on different welding parameters, Procedia Engineering 41 (2012) 1502-1506.
[10] N. Murugan, R.S. Parmar, Effects of MIG process parameters on the geometry of the bead in the automatic surfacing of stainless steel, Journal of Materials Processing Technology 41 (1994) 381-398.
[11] L.S. Rosado, T.G. Santos, M. Piedade, P. Vilaça, Advanced technique for non-destructive testing of friction stir welding of metals. Journal of Measurement 43 (2010) 1021-1030.
[12] T. Senthil Kumar, V. Balasubramanian, T. Senthilkumar, Influences of pulsed current tungsten inert gas welding on the tensile properties of AA 6061 aluminium alloy, Materials and Design 28 (2007) 2080-2092.
[13] K. Seshank, S.R.K. Rao, Y. Singh, K.P. Rao, Prediction of bead geometry in pulsed current gas tungsten arc welding of aluminium using artificial neural networks, Proceedings of International Conference on Information and Knowledge Engineering, IKE, Las Vegas, USA, 2003, 149-153.
[14] K. Sittichai, N. Santirat, P. Sompong, A study of gas metal arc welding affecting mechanical properties of austenitic stainless steel AISI 304, World Academy of Science, Engineering and Technology 61 (2012) 402-405.
[15] S. Datta, A. Bandyopadhyay, P.K. Pal, Grey-based Taguchi method for optimization of bead geometry in submerged arc bead-on-plate welding, International Journal of Advanced Manufacturing Technology 39 (2008) 1136-1143.
[16] S.C. Juang, Y.S. Tarng, Process parameters selection for optimizing the weld pool geometry in the tungsten inert gas welding of stainless steel, Journal of Materials Processing Technology 122 (2002) 33-37.
[17] Y.S. Tarng, W.H. Yang, Optimization of the weld bead geometry in gas tungsten arc welding by the Taguchi method, International Journal of Advanced Manufacturing Technology 14 (1998) 549-554.
[18] Y.S. Tarng, W.H. Yang, S.C. Juang, The use of fuzzy logic in the Taguchi method for the optimisation of the submerged arc welding process, International Journal of Advanced Manufacturing Technology 16 (2000) 688-694.
[19] Y.S. Tarng, S.C. Juang, C.H. Chang, The use of grey-based Taguchi methods to determine submerged arc welding process parameters in hard facing, Journal of Materials Processing Technology 128/1-3 (2002) 1-6.
[20] R. Yilmaz, H. Uzun, Mechanical properties of austenitic stainless steels welded by GMAW and GTAW, Journal of Marmara for Pure and Applied Sciences 18 (2002) 97-113.
[21] P.N. Rao, Manufacturing Technology, Volume 1, 3rd Edition, Tata McGraw-Hill Publishing Company Limited, 2009, 419.
[22] Causes for Weld Defects, IIW Doc. XII-B-046-83, International Institute of Welding, 1983.
[23] G. Rihar, M. Taucer, Lack of Fusion in Welded Joints, Varilna tehnika 51/4 (2002) 107-110 (in Slovenian).
[24] Gas-Shielded Metal-Arc Welding of Steel, IIW Doc. XII-B-049-83, International Institute of Welding, 1983.
[25] K. Sathishkuma, R. Vijaykumar, R. Rajmurugan, Study on defects in straight tube butt welding, International Journal of Scientific Engineering and Applied Science (IJSEAS) 1/5 (2015) 2395-3470.
[26] R.S. Parmar, Welding Processes and Technology, 2nd Edition, Khanna Publications, New Delhi, 1997.
[27] O.P. Khanna, Welding Technology, Dhanpat Rai & Sons, 1986.